

A large sample of low surface brightness disk galaxies from the SDSS. I: The sample and the stellar populations

G. H. Zhong,^{1,2*} Y. C. Liang,^{1†} F. S. Liu,^{4,1} F. Hammer,³ J. Y. Hu,¹ X. Y. Chen,¹
L. C. Deng¹ and B. Zhang^{2,1}

¹National Astronomical Observatories, Chinese Academy of Sciences, 20A Datun Road, Chaoyang District, Beijing 100012, China

²Department of Physicals, Hebei Normal University, Shijiazhuang 050016, China

³GEPI, Observatoire de Paris-Meudon, 92195 Meudon, France

⁴College of Physics Science and Technology, Shenyang Normal University, Shenyang 110034, China

Accepted 2008 Sep.17 Received 2008 Sep. 16

ABSTRACT

We present the properties of a large sample (12,282) of nearly face-on low surface brightness (LSB) disk galaxies selected from the main galaxy sample of SDSS-DR4. These properties include B -band central surface brightness $\mu_0(B)$, scale lengths h , integrated magnitudes, colors, and distances D . This sample has $\mu_0(B)$ values from 22 to 24.5 mag arcsec⁻² with a median value of 22.42 mag arcsec⁻², and disk scale lengths ranging from 2 to 19 kpc. They are quite bright with M_B taking values from -18 to -23 mag with a median value of -20.08 mag. There exist clear correlations between $\log h$ and M_B , $\log h$ and $\log D$, $\log D$ and M_B . However, no obvious correlations are found between $\mu_0(B)$ and $\log h$, colors etc. The correlation between colors and $\log h$ is weak even though it exists. Both the optical-optical and optical-NIR color-color diagrams indicate that most of them have a mixture of young and old stellar populations. They also satisfy color-magnitude relations, which indicate that brighter galaxies tend generally to be redder. The comparison between the LSBGs and a control sample of nearly face-on disk galaxies with higher surface brightness (HSB) with $\mu_0(B)$ from 18.5 to 22 mag arcsec⁻² show that, at a given luminosity or distance, the observed LSB galaxies tend to have larger scale lengths. These trends could be seen gradually by dividing both the LSBGs and HSBGs into two sub-groups according to surface brightness. A volume-limited sub-sample was extracted to check the incompleteness of surface brightness. The only one of the property relations having an obvious change is the relation of $\log h$ versus $\mu_0(B)$, which shows a correlation in this sub-sample.

Key words: galaxies: distances and redshifts - galaxies: fundamental parameters - galaxies: photometry - galaxies: spiral - galaxies: stellar content

1 INTRODUCTION

Low surface brightness galaxies (LSBGs) are galaxies that emit much less light per area than normal galaxies. Yet, owing to their faintness compared with the night sky, they are hard to find. Hence their contribution to the local galaxy population has been underestimated for a long time. It has been suggested that LSBGs may comprise up to half of the local galaxy population (McGaugh et al. 1995).

The discovery and searching history of the LSBGs and the understanding on them have been summarized by Impey & Bothun (1997) and Bothun et al. (1997). The first quantitative suggestion about LSBGs is the so-called Freeman’s

law. It was noticed by Freeman (1970) that the central surface brightness of 28 out of 36 disk galaxies fell in the range of $\mu_0(B)=21.65\pm 0.3$ mag arcsec⁻². This could be caused by selection effects (Disney 1976; Zwicky 1957).

The successful hunting for very diffuse galaxies (Romanishin et al. 1983 (from UGC); Sandage et al. 1984; Ellis et al. 1984; Bothun et al. 1987) prompted some new surveys. The first one was based on the second Palomar Sky Survey (POSS-II, Schombert and Bothun 1988; Schombert et al. 1992). A second one was initiated in the Fornax cluster using the Malinization technique in order to compare the results to Virgo (Bothun et al. 1992; Caldwell & Bothun 1987). The third one used the Automated Plate Measuring (APM) to scan UK Schmidt plates using an algorithm optimized to find LSB galaxies. This formed the most extensive catalog of LSB galaxies to that date (Impey et al. 1996). Morshidi-

* E-mail: ghzhong@bao.ac.cn

† E-mail: ycliang@bao.ac.cn

Esslinger et al. (1999a,b) extended such sample. The “Texas survey” (O’Neil et al. 1997a,b) increases the surface density of LSBGs in the general field, in which they firstly found the red LSB galaxy populations.

Following these catalogs, various aspects of LSBGs have been investigated. Especially, in a series of publications, Impey and his colleagues analyzed their APM survey sample (693 field galaxies in various morphologies, see Impey et al. 1996; Sprayberry et al. 1996; Sprayberry et al. 1997; Impey et al. 2001; Burkholder et al. 2001). Numerous other studies about LSBGs have been done based on smaller samples, relating to surface photometry and color distributions (McGaugh & Bothun 1994; de Blok et al. 1995; O’Neil et al. 1997a); number, luminosity and mass density (McGaugh 1996); AGN properties (Mei et al. 2008); and in the optical (Beijersbergen et al. 1999; Bergvall et al. 1999; Galaz et al. 2006, Zackrisson et al. 2005, Pizzella et al. 2008), near-IR (NIR, Bergvall et al. 1999; Galaz et al. 2002,2006; Monnier Ragaigne et al. 2003, Zackrisson et al. 2005), infrared (Hinz et al. 2007) and UV (Boissier et al. 2008) wavelengths. In addition, Kniazev et al. (2004) developed a method to search for LSBGs from modern survey and used the sample of Impey et. al. (1996) to test their method.

These studies show that LSBGs may be unevolved systems with low metallicity (McGaugh 1994; de Blok & van der Hulst 1998a; O’Neil et al. 1998; Bell et al. 2000), low stellar formation rate (van der Hulst et al. 1993; van Zee et al. 1997), small stellar density, a relatively high gas fraction (de Blok et al. 1996; McGaugh & de Blok 1997) and large amounts of dark matter (de Blok & McGaugh 1997). Despite these impressive progresses, there are still several challenges about LSBGs, such as many aspects of their formation and evolution, in particular, considerable uncertainty regarding their star formation history and so on. Moreover, the previous studies were based on small samples, up to about several hundreds, while the present modern digital sky surveys, such as the Sloan Digital Sky Survey (SDSS), greatly improved the observed numbers of astronomical objects, and could provide a much larger sample of LSBGs, hence giving much more information. Therefore, we propose a project to search for a large sample of LSBGs from the SDSS database, and then to study their properties in detail.

In this first paper of our series about the large sample of LSBGs selected from the SDSS, we will present how to select the sample and then show their basic properties and stellar populations from photometric colors. Then, we will present their spectroscopic properties (Liang et al. 2008, Chen et al. 2008, in preparation) and their detailed surface photometry and color gradients (Zhong et al. 2008, in preparation) etc. This paper is organized as follows. In Sect. 2, we describe how to select the sample. In Sect.3, we present the relations between some property parameters. In Sect.4, we compare the LSBGs with the HSB disk galaxies sample selected simultaneously. In Sect.5, we discuss the incompleteness of the sample at the low surface brightness end and present the property relations of a volume-limited sub-sample. In Sect.6, we do cross correlation for the sample with the 2MASS database to obtain their optical and NIR color-color diagrams and the color-magnitude relations. The discussions and conclusions are given in Sect.7. Throughout the paper, a cosmological model with $H_0=70 \text{ km s}^{-1} \text{ Mpc}^{-1}$,

$\Omega_M=0.3$ and $\Omega_\Lambda=0.7$ is adopted. The units of surface brightness is mag arcsec^{-2} .

2 THE SAMPLE

The SDSS is the most ambitious astronomical survey ever undertaken in imaging and spectroscopy (York et al. 2000; Stoughton et al. 2002; Abazajian et al. 2003, 2004). The imaging data are done in drift scan mode and are 95% complete for point sources at 22.0, 22.2, 22.2, 21.3, and 20.5 in five bands (u , g , r , i and z) respectively. The spectra are flux- and wavelength-calibrated with 4096 pixels from 3800 to 9200 Å at $R \approx 1800$.

The sample used in this work is selected from the main galaxy sample (MGS) of SDSS-DR4 (Strauss et al. 2002), which comprises galaxies with r -band Petrosian magnitude $r \leq 17.77$ (corrected for foreground Galactic extinction using the reddening maps of Schlegel et al. 1998) and r -band Petrosian half-light surface brightness $\mu_{50} \leq 24.5 \text{ mag arcsec}^{-2}$. This sample has a median redshift of about 0.10.

The MGS is a spectroscopic sample selected from the SDSS photometric data. The completeness for objects with spectroscopy observations is high, exceeding 99%, and the fraction of galaxies eliminated by surface brightness cut is very small ($\sim 0.1\%$). The only significant source of incompleteness identified is bending with saturated stars, which is higher for higher brightness because they subtend more sky (Strauss et al. 2002). Relative to all the SDSS targets, the SDSS spectroscopic survey is 90% complete (Blanton et al. 2003; Hogg et al. 2004; Strauss et al. 2002; McIntosh et al. 2006). The 7% incompleteness coming primarily from galaxies missed due to fiber collisions since the minimum separation of fiber centers is $55''$ (Blanton et al. 2003). It does lead to a slight underrepresentation of high-density regions (Hogg et al. 2004), however, where bright early-type galaxies usually dominate. Additionally, there are a small fraction of redshift failures ($\sim 1\%$) and some bright star contamination ($\sim 2\%$) that becomes more significant for brighter galaxies (Strauss et al. 2002; McIntosh et al. 2006). However, the completeness of the sample at the low surface brightness end needs to be discussed carefully because of the known problem of surface brightness limit in a redshift survey and the focus of our work on the low surface brightness ones. We will specially discuss this incompleteness in Sect. 5 and will extract a volume-limited sub-sample, which is complete, from our whole sample galaxies to check what changes appearing in the related properties of the galaxies.

We prefer to use the DR4 rather than the latest DR6 here. That is because DR4 has been large enough for statistical analysis of LSBGs; other property parameters for galaxies in DR4 have also been obtained by the MPA/JHU group¹, such as the emission-line measurements etc.; and the NYU-VAGC² catalog (Blanton et al. 2005) has made some useful cross correlations with other survey databases. These can provide us more information on both photometry and spectroscopy. Our sample galaxies are selected as follows.

¹ <http://www.mpa-garching.mpg.de/SDSS/>

² <http://sdss.physics.nyu.edu/vagc/>

2.1 The whole sample: the nearly face-on disk galaxies

To obtain reliable surface brightness values of the disk galaxies and minimize the effect of dust extinction inside the galaxies, we select the nearly face-on disk galaxies as a working sample by following the criteria below.

(i) $fracDev_r < 0.25$

The parameter $fracDev_r$ indicates the fraction of luminosity contributed by the de Vaucouleurs profile relative to exponential profile in the r -band. The topic in this work focuses on disk galaxies, whose surface brightness profiles usually can be well described by an exponential formula (e.g., Bernardi et al. 2005; Chang et al. 2006b; Shao et al. 2007). Therefore, we select the sample galaxies almost having an exponential light profile by requiring their $fracDev_r < 0.25$. This can minimize the effect of bulge light on the disk galaxies. Using this selection criterion, we can obtain 111,479 ($\sim 28\%$) objects from the total 401,007 galaxies in the SDSS-DR4 main galaxy sample.

(ii) $b/a > 0.75$

To select nearly face-on galaxies, we also require objects with the axis ratio $b/a > 0.75$ (corresponding to the inclination $i < 41.41$ degree), where a and b are the semi-major and semi-minor axes of the fitted exponential disk respectively. After this step is applied, 32,226 ($\sim 29\%$ of 111,479) galaxies are left.

(iii) $M_B < -18$

Keeping the B -band absolute magnitude $M_B < -18$ in mind excludes the few dwarf galaxies contained in the sample. The B -band absolute magnitude M_B is calculated using

$$M = m - 5 \log(D_L) - K(z), \quad (1)$$

where m is the apparent magnitude that corrected for Galactic extinction using the reddening maps of Schlegel et al. (1998), D_L is the luminosity distance calculated by using the Local Group relative redshift values from the NYU-VAGC catalog (Blanton et al. 2005, see Sect. 3.1). The K -correction $K(z)$ are calculated by using the K -corrections program given on the NYU-VAGC website (Blanton et al. 2005). Finally, we obtain 30,333 galaxies as our whole sample after excluding $\sim 6\%$ of 32,226 nearly face-on disk galaxies by this criterion.

2.2 The subsamples: the LSBGs and HSBGs

A commonly used parameter to classify a galaxy to be one with low (or high) surface brightness is its B -band central surface brightness $\mu_0(B)$. In this work, we adopted $\mu_0(B) \geq 22$ mag arcsec $^{-2}$, a commonly applied criterion (Boissier et al. 2003), as LSBGs and $\mu_0(B) < 22$ mag arcsec $^{-2}$ as high surface brightness galaxies (HSBGs) following Impy, Burkholder & Sprayberry (2001) and O'Neil et al. (1997a,b).

The surface brightness profiles of disk galaxies are well approximated by an exponential disk profile with the form:

$$\Sigma(r) = \Sigma_0 \exp\left(-\frac{r}{a}\right), \quad (2)$$

where Σ_0 is the surface brightness of the disk in units of $M_\odot \text{ pc}^{-2}$ and a is the disk scale-length measured in units of arcsec. In the logarithmic units, this equation becomes:

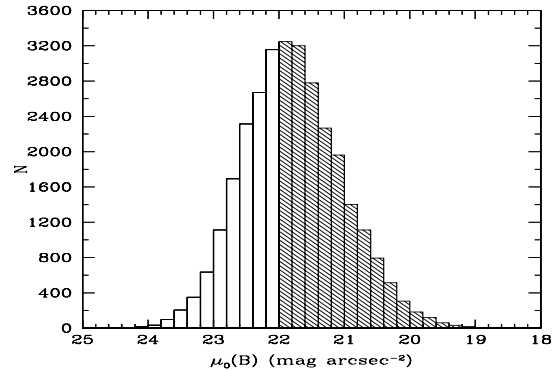


Figure 1. Histogram distribution of the selected nearly face-on disk galaxies (30,333) in B -band central surface brightness $\mu_0(B)$. The whole sample is divided into two parts: the white region with $\mu_0(B) \geq 22$ mag arcsec $^{-2}$ as the LSBGs (12,282), and the shadowed region with $\mu_0(B) < 22$ mag arcsec $^{-2}$ as the HSBGs (18,051).

$$\mu_r = \mu_0 + 1.086 \left(\frac{r}{a}\right), \quad (3)$$

where μ_0 is the central surface brightness in mag arcsec $^{-2}$.

In the analysis, the disk is assumed to be infinitely thin. The total flux is given by:

$$F_{tot} = 2\pi a^2 \Sigma_0. \quad (4)$$

Then, the total apparent magnitude can be determined from this equation. Converting this to a logarithmic scale is:

$$\mu_0 = m + 2.5 \log(2\pi a^2), \quad (5)$$

where m refers to the total apparent magnitude and μ_0 refers to the central surface brightness.

The central surface brightness is corrected by inclination and cosmological dimming effects by following:

$$\mu_0 = m + 2.5 \log(2\pi a^2) + 2.5 \log(b/a) - 10 \log(1+z), \quad (6)$$

where z is the redshift of the target.

The B -band (also U , V , R) central surface brightnesses and magnitudes of the SDSS galaxies can be calculated from the g and r -band quantities by using the conversions provided by Smith et al. (2002). The histogram distribution of $\mu_0(B)$ for our selected whole sample (30,333 galaxies) is shown in Fig. 1. The blank histogram is for the LSBGs and the shadowed one is for the HSBGs with the separating value of 22 mag arcsec $^{-2}$. We call the LSBGs as **Sample-L** and the HSBGs as **Sample-H** in this work. Sample-L includes 12,282 ($\sim 40\%$) galaxies with $22 \leq \mu_0(B) \leq 24.5$ mag arcsec $^{-2}$ with median and mean values of 22.42 and 22.50 mag arcsec $^{-2}$ respectively. Sample-H includes 18,051 ($\sim 60\%$) galaxies with $18.5 \leq \mu_0(B) < 22$ mag arcsec $^{-2}$ with median and mean values of 21.41 and 21.29 mag arcsec $^{-2}$ respectively. Since the LSBGs are the major topic of this paper, we will carefully present the properties of Sample-L in Sect. 3 and roughly compare the HSBGs with the LSBGs in Sect. 4. However, when looking for the relations of some property parameters with surface brightness, it is useful to show all of the sample, including LSBGs and HSBGs, therefore, in Sect.3.2 we present both the LSBGs and HSBGs in the relations of m_B , distance, M_B with $\mu_0(B)$. The

cross-correlations with near infrared 2MASS data will be emphasized in Sect. 6.

3 PROPERTY PARAMETERS AND RELATIONS OF THE LARGE SAMPLE OF LSBGS

Some property parameters of LSBGs have been obtained and discussed in previous work, such as Impey et al. (1996, 2001), de Blok et al. (1995), Bothun et al. (1997), Galaz et al. (2002, 2006) etc. In this section, we present some property parameters and relations for our Sample-L (the LSBGs) and compare them with the previous results. The Sample-H (HSBGs) are also given in the relations of m_B , distance, M_B with $\mu_0(B)$ (see Sect.3.2 and Fig. 3), which is useful to show the entire sample.

3.1 The histogram distributions of some property parameters

We show the distributions of some property parameters of our LSBGs in Fig. 2. Fig. 2a shows the histogram distribution of their redshift z obtained from the NYU-VAGC catalog (Blanton et al. 2005), which are the peculiar velocity corrected Local Group relative redshifts from SDSS. It shows that the redshifts are from 0 to 0.3 with median and mean values of 0.080 and 0.089, respectively. Fig. 2b shows the histogram distributions of the disk scale-length a in arcsec, and Fig. 2c shows the histogram distributions of the disk scale-length h in kpc. The range of a is from 2 to 13 arcsec with median and mean values of 3.78 and 4.19 arcsec, and h is from 2 kpc to 19 kpc with median and mean values of 5.98 and 6.30 kpc, respectively. The scale lengths of LSBGs investigated here are in the same ranges as in McGaugh (1992) and de Blok et al. (1995). Fig. 2d shows the histogram distribution of the B -band absolute magnitudes, which is calculated using Eq. (1). It shows that the LSBGs are not necessary faint galaxies, but rather they are quite bright, M_B is from -18 to -23 mag with the median and mean values of -20.08 and -20.06 mag, respectively.

3.2 Distributions of some property parameters with B -band central surface brightness

We present the relations between the total B -band apparent magnitudes, distance, absolute magnitude M_B and the B -band central surface brightness $\mu_0(B)$ for Sample-L and Sample-H.

3.2.1 central surface brightness and apparent magnitude

Figure 3a presents the relations between the B -band apparent magnitudes and the B -band central surface brightness $\mu_0(B)$. The vertical lines separate the LSBGs and HSBGs with $\mu_0(B)=22$ mag arcsec $^{-2}$. It shows that these galaxies have the m_B from 14 to 19 mag. At a given magnitude, most galaxies are detectable over a wide range of surface brightnesses, for example, $18 < \mu_0(B) < 24.5$ mag arcsec $^{-2}$ at $m_B=18$ mag. There exists almost no correlation within the ranges. Some objects missed probably at faint μ_0 could be

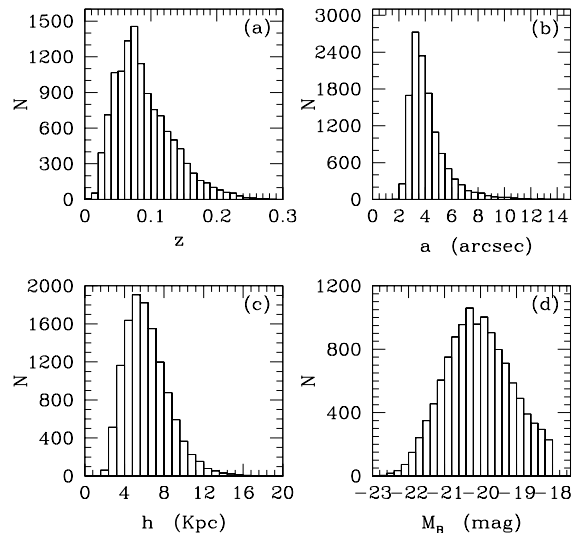


Figure 2. Histogram distributions of some property parameters of Sample-L (the LSBGs): (a). the redshift, obtained from NYU-VAGC catalog and is the peculiar velocity-corrected Local Group relative redshift from SDSS; (b). the disk scale length (the disk semi-major axis) in arcsec as a ; (c). the disk scale length (the radius) in kpc as h ; (d). the B -band absolute magnitude M_B , which obviously shows that LSBGs does not necessarily have low luminosity, and the LSBGs can be very luminous.

due to the poor contrast with the sky brightness. These results are similar to those shown by the samples of APM survey (693 LSB field galaxies) given by Impey et al. (1996).

3.2.2 central surface brightness and distance

Figure 3b presents the distribution of the distance versus $\mu_0(B)$ of the sample galaxies. For the LSBGs, the left part of the vertical line, it shows that the range of surface brightness for the nearest galaxies is substantially larger than that for the more distant galaxies. We expect this to influence surface brightness selection, where galaxies with higher surface brightness could be seen at the largest distances (Disney & Phillips 1983, Impey et al. 1996). But for the HSBGs, the right part of the vertical line, it does not obviously show such trend. This may mean that the selection bias affects much the LSBGs. This distribution is consistent with that of the sample in the APM survey presented by Impey et al. (1996). However, the volume-limited sub-sample of LSBGs do not show such a trend (see Sect.5).

3.2.3 central surface brightness and absolute magnitude

Figure 3c presents the distribution of the absolute B -band magnitudes versus $\mu_0(B)$ of the sample galaxies. The left part from the vertical line is for the LSBGs. There exists a correlation among them showing that the fainter galaxies tend to have lower surface brightnesses though there is large scatter. It also shows over the whole range of $22 < \mu_0(B) < 24.5$ mag arcsec $^{-2}$, galaxies are being discovered over the entire range of $-23 < M_B < -18$ mag. The right part from the vertical line is for the HSBGs, which show that

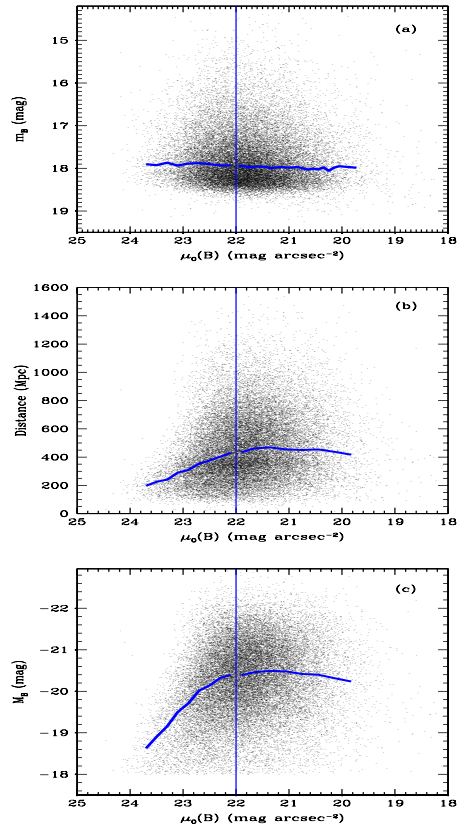


Figure 3. Distributions of some property parameters with $\mu_0(B)$ for our LSBGs (the left part of the vertical line) and HSBGs (the right part of the vertical line): (a). the total B -band apparent magnitudes; (b). the distance of the galaxies; (c). the B -band absolute magnitudes. The solid lines are the median-value points within the bins of 0.10 of $\mu_0(B)$ less than $23.6 \text{ mag arcsec}^{-2}$, and we take $\mu_0(B)$ greater than $23.6 \text{ mag arcsec}^{-2}$ as one bin because there are very few sources. The lines refer to the median-value points within the bins.

there is no obvious correlation between their M_B and $\mu_0(B)$. This could mean that the selection bias affects the LSBGs greatly. These are also similar to that presented by the APM sample given by Impey et al. (1996).

3.3 Distributions of some property parameters with disk scale length and distance

Some of the previous studies have shown there are obvious correlations between the luminosity and disk scale length $\log h$ (Impey et al. 2001; Bergvall et al. 1999), distance $\log D$ and disk scale length $\log h$ (Impey et al. 2001) for LSBGs. These relations become more clear from our much larger and homogeneous sample.

3.3.1 disk scale length and luminosity

We show the relation between absolute magnitudes M_B and disk scale length $\log h$ for our Sample-L in Fig. 4. It can be seen that there is a very clear correlation between them, which can be fitted by a least-square fit as

$$\log h = -0.150(\pm 0.0007)M_B - 2.245(\pm 0.014), \quad (7)$$

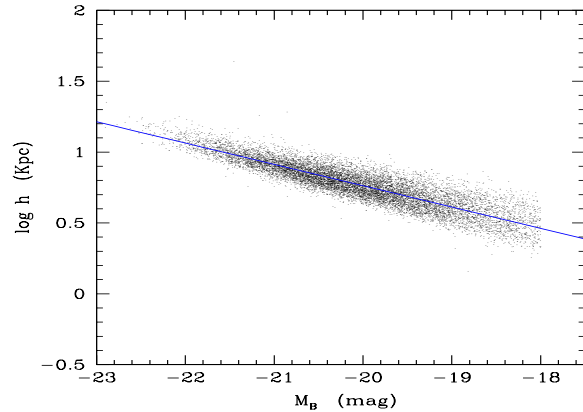


Figure 4. Relations of the LSB sample galaxies about their disk scale length in logarithm versus B -band absolute magnitudes. The solid line refers to the least-square fit for the sample galaxies given by Eq.(7). The Spearman-Rank Order correlation coefficient is -0.893 .

with a small standard deviation of 0.070 dex. The Spearman-Rank Order correlation coefficient is -0.893 .

This correlation has been shown in Impey et al. (2001, for their 238 galaxies from APM) and Bergvall et al. (1999, for the gathered samples from literature), but is more obvious for our larger and homogeneous sample. It shows brighter galaxies tend to have larger scale lengths.

It is worth comparing such relations of our LSBGs with the corresponding relations of HSBGs. They show some discrepancies, which will be specially discussed in Sect. 4.

3.3.2 disk scale length and distance

Our LSBGs sample also show a very clear correlation between their distance and disk scale length, which is given in Fig. 5. This correlation can be given by a least-square fit as:

$$\log h = 0.511(\pm 0.004) \log D - 0.536(\pm 0.010), \quad (8)$$

with the standard derivation of 0.10 dex. The Spearman-Rank Order correlation coefficient is 0.767.

This relation obviously show the selection effect, i.e., in the more distant Universe, the galaxies with larger scale lengths have the benefit that they can be detected and observed.

3.3.3 distance and luminosity

Figure 6 shows the distribution between the distance $\log D$ and the B -band absolute magnitude M_B . It could be seen that there is an obvious correlation between them, though there is some scatter. This correlation can be shown by a least-square fit as:

$$\log D = -0.211(\pm 0.001)M_B - 1.675(\pm 0.025), \quad (9)$$

with the standard derivation of 0.13 dex. The Spearman-Rank Order correlation coefficient is -0.847 .

This correlation show the selection effects of the survey observation. That means the brighter galaxies can be observed at larger distances, and the relatively fainter ones can only be observed at smaller distances.

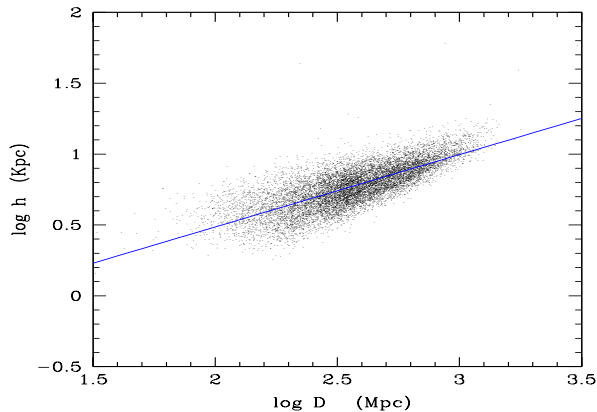


Figure 5. Relations of the LSB sample galaxies about their distance versus disk scale length. The solid line refers to the least-square fit for the sample galaxies given by Eq.(8). The Spearman-Rank Order correlation coefficient is 0.767.

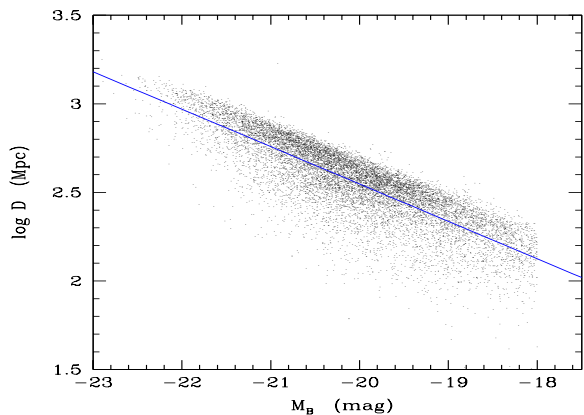


Figure 6. Distribution of the distance $\log D$ and the B -band absolute magnitude M_B for our LSBGs. The solid line refers to the least-square fit for the sample galaxies given by Eq.(9). The Spearman-Rank Order correlation coefficient is -0.847.

3.3.4 disk scale lengths and central surface brightness

Figure 7 shows the distribution between disk scale length $\log h$ and the central surface brightness $\mu_0(B)$, which does not show obvious correlation. This result is consistent with those of Beijerbergen et al. (1999) and O’Neil et al. (1997b) for smaller samples.

3.4 Relations between colors and disk scale length, colors and central surface brightness

In this section we show the relations between colors and disk scale length, as well as between colors and central surface brightness for the LSBGs.

3.4.1 colors and disk scale lengths

Figure 8a presents the distribution between $(B - V)$ color and disk scale length of our large sample of LSBGs. The correlation between them is weak even though it exists, and

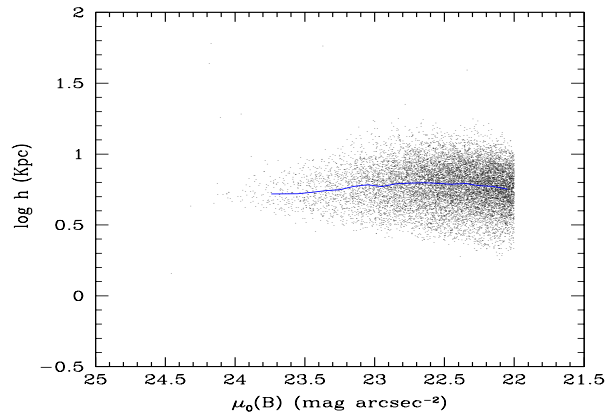


Figure 7. Distribution of the disk scale length versus the B -band surface brightness for our LSBGs. The solid line is the median-value points within the bins that is the same as Fig. 3.

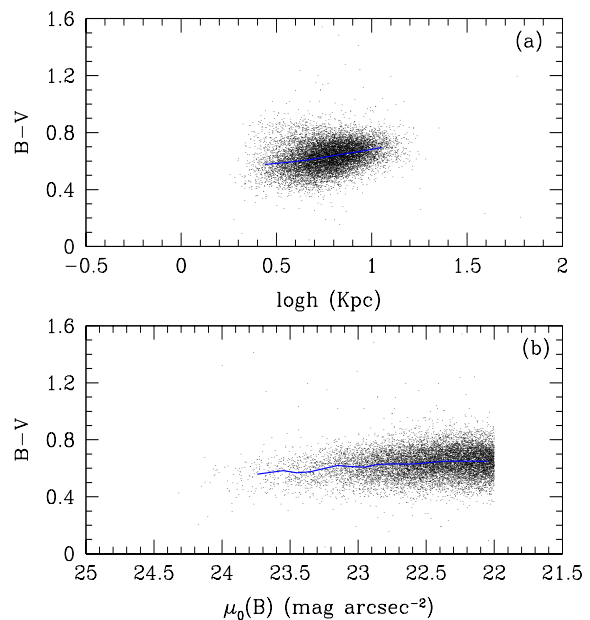


Figure 8. (a). Distribution of $B - V$ color as a function of disk scale length for the Sample-L. The solid line is the median-value points within the bins of 0.10 of $\log h$ from 0.5 to 1.0 (h in kpc). But $\log h$ less than 0.5 or greater than 1.0 (h in kpc) as one bin, respectively, since the sources are very few in those two bins. (b). Distribution of $B - V$ color as a function of B -band central surface brightness for the Sample-L. The solid line is the median-value points within the bins that is same as Fig. 3.

the Spearman-Rank Order correlation coefficient between them is only 0.302. Our result is not much different from the previous studies on small samples (e.g., de Blok et al. 1995; Beijersbergen et al. 1999), which showed the colors do not depend on sizes of LSBGs. But Bergvall et al. (1999) have showed an obvious correlation for a small sample of spirals, large LSBGs and their blue LSBGs.

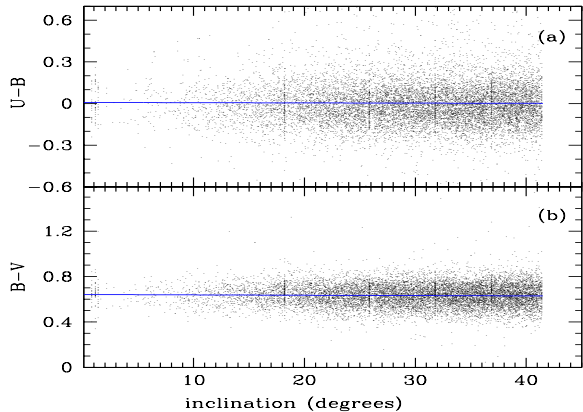


Figure 9. Relations between disk inclination and colors of the Sample-L: (a). $U - B$, (b). $B - V$. The solid lines are the least-square fits for the data, which show almost no slopes.

3.4.2 colors and central surface brightness

Figure 8b presents the distribution between the $(B - V)$ colors and central surface brightness $\mu_0(B)$ for our Sample-L, which does not show obvious correlation in the whole ranges of the two parameters. The results presented from smaller samples of LSBGs studied by Beijersbergen et al. (1999), de Blok et al. (1995) and Bothun et al. (1997) are consistent with our result here from a large sample of LSBGs.

3.5 The optical color-color diagram and stellar populations

3.5.1 The negligible affect of dust extinction on colors

In this work, we have selected the nearly face-on disk galaxies to minimize the affection of dust extinction. Thus their properties of stellar population won't be affected much by dust extinction, which could be confirmed by the independence of the colors with inclination. Fig. 9 shows such independence of the LSB sample galaxies (12,282). Indeed the HSB sample galaxies present similar independence, which were not presented as plots here to save space. Additionally, we also do cross-correlations for these nearly face-on disk galaxies with the IRAS infrared PSCz catalog within a range of 5 arcsec, but only find very few IR-detected objects, which also confirm the negligible affect of dust on their properties. This negligible affect of dust on colors is consistent with other studies (e.g., Bell et al. 2000; Galaz et al. 2006).

3.5.2 UBV diagram and stellar populations

O'Neil et al. (1997a,b) have performed a digital survey for LSBGs in the spiral-rich Cancer and Pegasus clusters as well as the low density regime defined by the Great Wall (the "Texas survey"). They found a total of 127 galaxies of angular diameter larger than 15 arcseconds with $\mu_0(B) \geq 22$ mag arcsec⁻². They discussed the stellar populations of this sample of LSBGs by optical color-color relations and firstly found the very red population of LSBGs. They divided the galaxies into three categories: the very blue (with $(U - B) <$

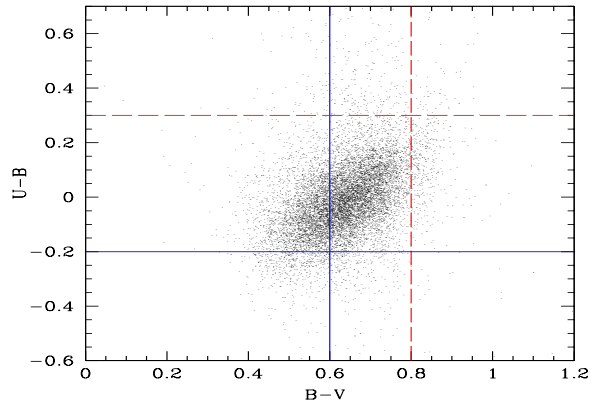


Figure 10. $U - B$ versus $B - V$ diagram of our LSBGs. The solid and dashed lines are taken from O'Neil et al. (1997b) to define the "very blue" and "very red" populations of galaxies (see text).

$-0.2, (B - V) < 0.6$), the very red (with $(U - B) > 0.3, (B - V) > 0.8$), and the rest that have other color values.

In our Fig. 10, we shows the $(U - B)$ vs. $(B - V)$ diagram for our Sample-L. The average values of our sample galaxies are $\langle (U - B) \rangle = -0.0012 \pm 0.08$, $\langle (B - V) \rangle = 0.64 \pm 0.06$ in the ranges of $-0.6 \leq (U - B) \leq 0.6$ and $0 \leq (B - V) \leq 1.2$. These are not very different from O'Neil's sample, and is similar to those of Romanishin et al. (1983) and McGaugh & Bothun (1994) as well.

We also plot the separation lines suggested by O'Neil et al. (1997a,b) for the "very blue" and "very red" LSBGs in Fig. 10 (the solid and dashed lines, see above). Our Sample-L contains 535 ($\sim 4.4\%$) "very blue" LSBGs and 69 ($\sim 0.48\%$) "very red" LSBGs. Most of the sample galaxies are the "rest case" with mixed stellar populations.

Heller & Brosch (2001) also present such UBV colors for their 29 LSB dwarf irregular galaxies from the Virgo cluster, and found their "very blue" is about 30% and no "very red" ones. These two different fractions could be easily understood since their samples are dwarf irregular galaxies, which should be blue. de Blok et al. (1995) also present such a UBV diagram for a small sample of 21 LSB galaxies gathered from literature, and they did not find any sample belonging to the "very red" range that O'Neil et al. suggested.

The colors of these LSBGs are obviously different from those of the E0/S0 galaxies but not much different from the Sc or later spiral galaxies with active star formation. As O'Neil et al. (1997b) commented, the average colors of E0/S0 galaxies (good examples of old stellar populations) have $(U - B) = 0.54$, $(B - V) = 0.96$ (Tinsley 1978); Sc or later spiral galaxies with active star formation typically have colors in the range of $0.35 \leq (B - V) \leq 0.65$, $-0.2 \leq (U - B) \leq 0.4$ (Huchra 1977; Bothun 1982), with mean values $\langle (B - V) \rangle \sim 0.50$, $\langle (U - B) \rangle \sim -0.20$ (Bothun 1982), and $\langle (V - I) \rangle \sim 1.0$ (Han 1992).

The colors of our galaxies range continuously from very blue to very red and include a group of old galaxies, which show evidence of recent star formation. These LSBGs at the present epoch define a wide range of evolutionary states. This wide range is similar to that of the high surface brightness galaxies (see Sect. 4).

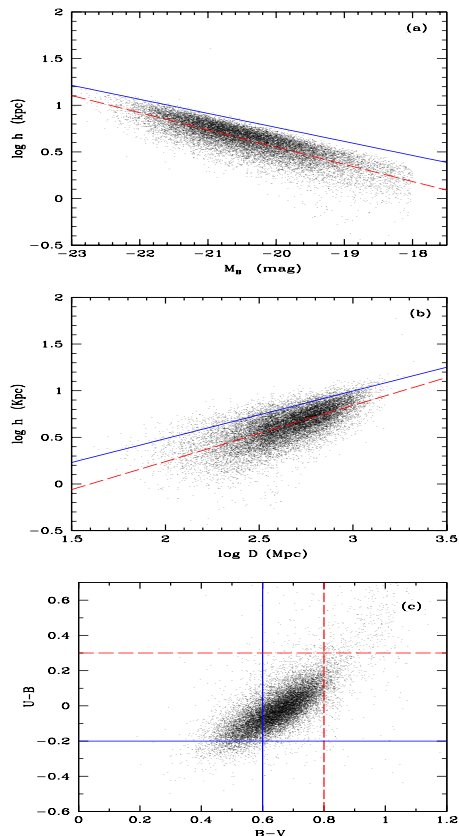


Figure 11. Some relations of HSBGs: (a). correlation of luminosity and disk scale length, the dashed line is the least-square fit for the data and the solid line is the fit for the LSBGs given in Fig.4; (b). correlation of distance and disk scale length, the dashed line is the least-square fit for the data and the solid line is the fit for the LSBGs given in Fig.5; (c). $U - B$ vs. $B - V$ color-color diagram, the solid and dashed lines are the same as in Fig.10.

4 COMPARISONS BETWEEN THE HSBGS AND THE LSBGS

In this section, we present the correlations between $\log h$ and M_B , $\log h$ and distance for HSBGs, and compare them with those of the LSBGs.

Figure 11a shows the clear correlation of luminosity and disk scale length for the HSBGs. This correlation can also be given by a least-square fit by the dashed line as:

$$\log h = -0.184(\pm 0.0009)M_B - 3.135(\pm 0.018), \quad (10)$$

with the standard deviation of 0.10 dex. The Spearman-Rank Order correlation coefficient is -0.846. The solid line refers to the corresponding least-square fit for the LSBGs given in Fig.4, which is shallower than the dashed line. The discrepancy between the solid and dashed lines means that at a given luminosity, the LSBGs need to be larger than the HSBGs if both of them can be detected and observed; and with a given disk scale length, the HSBGs are brighter than the LSBGs.

Figure 11b shows the correlation between the distance and disk scale length for the HSBGs. This correlation can be given by a least-square fit (the dashed line in the figure)

as:

$$\log h = 0.601(\pm 0.005) \log D - 0.961(\pm 0.012), \quad (11)$$

with the standard deviation of 0.14 dex. The Spearman-Rank Order correlation coefficient is 0.710. The same, the solid line refers to the least-square fit for the LSBGs. The discrepancy between the solid and dashed lines means that at a given distance, the LSBGs need to be larger than the HSBGs if they can be detected and observed, in another word, with a given disk scale length, the HSBGs could be observed at a farther distance.

Figure 11c shows the color-color diagram of $(U - B)$ and $(B - V)$ of the HSBGs. The ranges of the two colors are almost similar to those of the LSBGs, but the HSBGs show less scatter here. It also shows that the HSBGs have larger fraction of the “very red” objects than in the LSBGs, i.e., the fraction is 2.1%, higher than the 0.48% in the LSBGs, and the fraction of the “very blue” objects in the HSBGs is about 4.0%, which is a bit lower than the 4.4% in the LSBGs. This is acceptable since the HSBGs could have more older stellar populations than the LSBGs. The others are the mix of old and young stellar populations.

5 THE VOLUME-LIMITED SUB-SAMPLE

Since we are looking for the property relations of low surface brightness galaxies, it is important to discuss the completeness of the sample at the low surface brightness end. As Blanton et al. (2005b) discussed, the incompleteness at low surface brightness is due primarily to two effects. First, the inappropriate shredding by the photometric deblender of low surface brightness galaxies, which often relates to the presence of nearby stars. This shredding tends to reduce the galaxy fluxes to well below the flux limits of the survey. Second, for many galaxies the flux is significantly reduced because the sky subtraction determination subtracts a substantial fraction of the galaxy light.

Blanton et al. (2005b) discussed the contributions to completeness as a function of surface brightness, the r -band Petrosian half-light surface brightness $\mu_{50,r}$. In their Fig.3, they present the completeness of the SDSS photometric catalog, the tilling catalog (the SDSS spectroscopic targeting with respect to the photometric catalog), the redshift of the spectroscopy for targets that have been observed, and the total of these three. It shows that, for those brighter ones with $\mu_{50,r} < 23$ mag arcsec⁻², the completeness of the spectroscopy is very close to 100%, which is consistent with Strauss et al. (2002), who discussed the high completeness of the SDSS main galaxy sample. This $\mu_{50,r}$ cut just corresponds to $\mu_0(B) = 24.5$ mag arcsec⁻², which could be obtained from the fitted relation for our whole sample galaxies: $\mu_0(B) = 1.111 \times \mu_{50,r} - 1.274$. But for the photometric and tilling catalogs, they show obvious incompleteness within $\mu_{50,r} = 22-23$ mag arcsec⁻² (corresponding to $\mu_0(B)$ about 23.2-24.3 mag arcsec⁻²), then the total completeness there could decrease to be about 70%.

To avoid the effects of the incompleteness on the property relations derived from our sample galaxies, and to check that the obtained trends (Fig. 1-10) are real or arise from selection effects, we extract a volume-limited sub-sample from the $M_r - z$ plane by considering $z < 0.1$ and those brighter

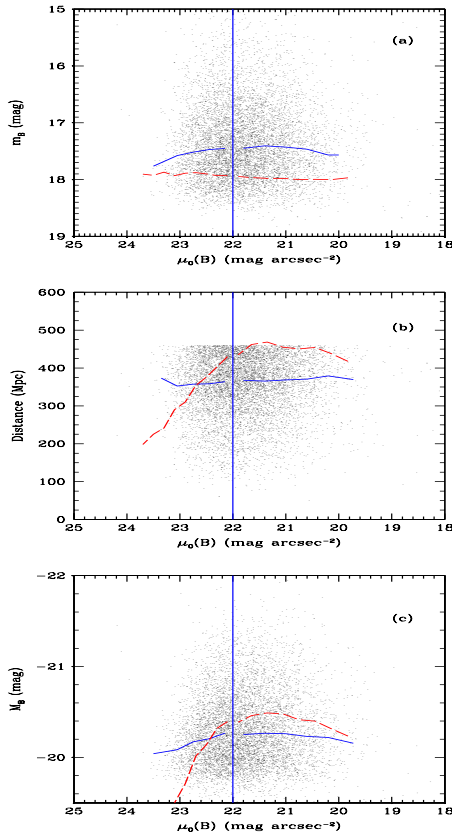


Figure 12. Distributions of the property relations of the volume-limited sub-sample corresponding to Fig. 3: (a). the total B -band apparent magnitudes with $\mu_0(B)$; (b). the distance of the galaxies with $\mu_0(B)$, the upper cut corresponds to the redshift cut, $z < 0.1$; (c). the B -band absolute magnitudes with $\mu_0(B)$. The solid lines are the median-value points within the bins of $\mu_0(B)$. The long-dashed lines are the same as Fig. 3.

ones than the corresponding M_r , and then re-obtain such relations, which are given by Fig. 12 and Fig. 13. This volume-limited sample includes 3313 LSBGs and 4722 HSBGs.

Corresponding to Fig. 3, Fig. 12 shows the distributions of this volume-limited sub-sample in the relations between m_B , distance, M_B and $\mu_0(B)$. This sub-sample is similar to that entire sample selected from magnitude in their relations of m_B and $\mu_0(B)$ (Fig. 12a). The upper cut of distance is the redshift cut of $z = 0.1$, and both of the LSBGs and HSBGs do not show correlations between distance and $\mu_0(B)$ now (Fig. 12b). For the LSBGs in this volume-limited sub-sample, there exists a weak correlation between M_B and $\mu_0(B)$, but no correlation for the HSBGs (Fig. 12c). However, because of the redshift cut and the corresponding M_r magnitude cut for this volume-limited sub-sample, some distant brighter objects and the nearby faint ones are lost from the entire sample, thus the range of M_B becomes narrower.

To further check whether the property relations of sample-L galaxies presented in Figs. 1,2,4-10 are kept or not in this volume-limited sub-sample, we re-obtained all the related plots. Fig. 13 shows some of them. Fig. 13a-d show the same histogram distributions as Fig. 2, but for the volume-limited sub-sample. They show that the median values of redshift, disk scale length a and h , B -band absolute magnitude are 0.079, 4.35 arcsec and 6.27 kpc, -20.21 mag,

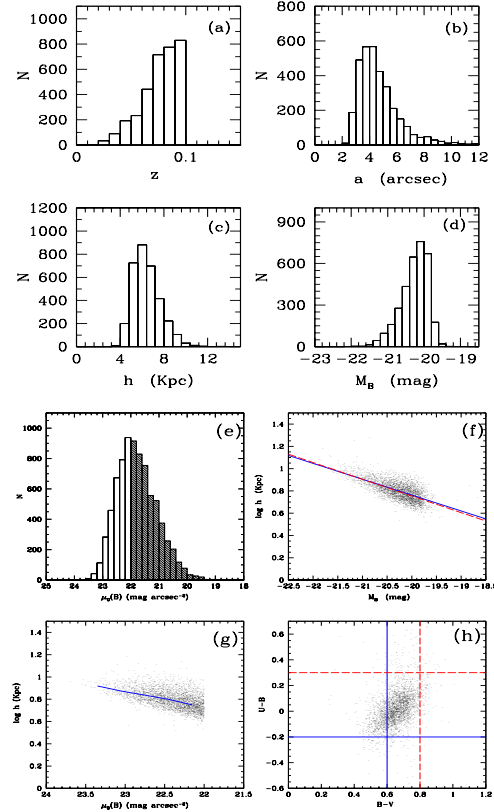


Figure 13. The property parameters of the LSBGs in the volume-limited sub-sample. (a-d) The same histogram distributions as Fig. 2a-d. (e). Histogram distribution of $\mu_0(B)$ (as Fig. 1), the blank histogram is for the 3313 LSBGs and the shadowed one is for the 4722 HSBGs with the separating value of 22 mag arcsec $^{-2}$. (f). Disk scale length vs. luminous, with the solid line as the linear least-square fit, and the long-dash line is the fit for the entire sample of LSBGs given in Fig. 4. (g). Distribution of disk scale length and central surface brightness, and the solid line is for the median-value points (as Fig. 7). (h). UBV color-color diagram (as Fig. 10).

respectively. Fig. 13e presents the histogram distribution of $\mu_0(B)$, which is similar to Fig. 1 for the entire sample, and with median values of 22.37 for the 3,313 LSBGs and 21.43 for the 4,722 HSBG, respectively. Fig. 13f shows the relations of $\log h$ versus M_B (the solid line refers to the linear least-square fit), which corresponds to Fig. 4 and is quite similar to that (the dashed-line). Fig. 13g shows that there is a correlation between $\log h$ and $\mu_0(B)$, which was not seen in Fig. 7 for the magnitude-limited sample galaxies. Fig. 13h show the $U - B$ vs. $B - V$ color-color diagram, which is quite similar to the magnitude-limited sample given in Fig. 10 and means that most of these LSBGs have mix of young and old populations. For other relations related to distance, it is not interesting to show the distribution because of the redshift (distance) cut. For the color vs. $\log h$ and $\mu_0(B)$ relations, this volume-limited sub-sample shows similar trends to our entire magnitude-limited LSBGs (Fig. 8), and the weak correlation in Fig. 8a disappear here. We did not present them as plots.

6 OPTICAL AND NEAR INFRARED SURFACE PHOTOMETRY AND STELLAR POPULATIONS OF LSBGS

The color-color diagram of galaxies can give some hints about their ages and metallicities and hence the stellar populations. But the well-known problem in this is the degeneracy of age and metallicity of galaxies. The recent studies show that the combination of optical and NIR colors could break this degeneracy. Thus several optical-NIR color-color diagrams have been used for this purpose for the LSB galaxies (Romanishin et al. 1982; Bergvall et al. 1999; Galaz et al. 2002, 2006; Bell et al. 1999, 2000; Monnier Ragainie et al. 2003; MacArthur et al. 2004; Bell & de Jong 2000 for spiral galaxies). In this section, we obtain and present the optical-NIR color-color diagram ($(R - K)$ vs. $(B - R)$ as an example) of our whole sample galaxies and show their stellar populations by comparing with the stellar population synthesis models with different metallicities and ages.

6.1 Cross correlation with 2MASS

The 2MASS is a ground-based, near-infrared full-resolution for each extended imaging survey of the whole sky and its Extended Source Catalog (XSC) contains almost 1.6 million galaxies (Skrutskie et al. 1997; Cutri et al. 2000; Jarrett et al. 2000a,b). 2MASS has imaged the entire celestial sphere in the near-infrared J (1.11-1.36 μ m), H (1.50-1.80) and K_s (2.00-2.32) bands (we use K hereafter) using two identical dedicated 1.3-meter telescopes for detecting brighter than 14th mag at K with angular diameters greater than ~ 10 arcsec. It has a 95% completeness level in J , H and K of 15.1, 14.3 and 13.5 mag, respectively.

The NYU-VAGC contains a matched sample between the SDSS and 2MASS XSC. We do cross-correlation between Sample-L (as well Sample-H) and the 2MASS-XSC catalog matched by NYU-VAGC with the error ellipse within 3 arcsec. The resulting samples are **Sample-L2** with 1,878 (15.29%) LSB galaxies and **Sample-H2** with 5,320 (29.47%) HSB galaxies, respectively. The fraction detected by the 2MASS NIR for the LSBGs is only half that of the HSBGs. This can be understood naturally because the galaxies with lower surface brightness could be lost more easily in a shallower survey, or due to their relatively bluer colors.

McIntosh et al. (2006) has carefully discussed the completeness of 2MASS. From the cross correlation with the main galaxy sample of the SDSS, they found that 2MASS detects 90% of SDSS galaxies brighter than $r = 17$ mag. These detections span the representative range of optical and near-infrared galaxy properties, but with a surface brightness-dependent bias that preferentially misses sources at the extreme blue and low-concentration end of parameter space, which are consistent with the most morphologically late-type galaxy population. An XSC completeness of 97.5% is achievable at bright magnitudes, with blue low-surface-brightness galaxies being the only major source of incompleteness. Even with this bias of surface brightness, our qualitative conclusion about the mix of stellar populations of LSBGs is still reasonable as will be discussed in Sect.5.2.

We should guarantee that the SDSS and 2MASS mag-

nitudes are measured within the same aperture when we obtain the optical-NIR colors of the galaxies. We adopt the method of Chang et al. (2006a,b) to do the aperture corrections for the magnitudes, i.e., to correct the SDSS magnitudes to the same aperture where the 2MASS magnitudes are measured. To do so, we firstly adopt the isophotal fiducial magnitudes of J , H and K magnitudes provided by the 2MASS, which are measured within the circular aperture corresponding to a surface brightness of 20.0 mag arcsec $^{-1}$ in the K -band. The aperture was denoted by R_{K20fc} . Then we use the *ProfMean* measurements provided by the SDSS to match the circular aperture of the R_{K20fc} in 2MASS. The *ProfMean* parameter is the azimuthally averaged surface brightness in a series of 15 circular annuli, which has been given in all the SDSS u, g, r, i, z photometric magnitudes. All the magnitudes are corrected for Galactic extinction and K -correction following the same method mentioned in Sect. 2.1.

6.2 Optical-NIR color-color diagram and stellar populations

In Fig. 14 we show the optical-NIR diagrams of $(R - K)$ vs. $(B - R)$: (a) for Sample-L2; (b) for Sample-H2. The overplots are the stellar population synthesis models obtained by Bell et al. (2000) using the GISSL98 implementation of the stellar population models of Bruzual & Charlot (2003), where the horizontal lines refer to the different metallicities and the vertical lines refer to the different characterized e-folding time-scale τ of their star formation. They adopted a Salpeter (1955) initial mass function (IMF) where the lower mass limit of the IMF was $0.1 M_{\odot}$ and the upper mass limit was $125 M_{\odot}$, and an exponentially decreasing star formation rate characterized by an e-folding time-scale τ and a single, fixed stellar metallicity Z . Given the joint evidence of the WMAP that the last electron scatter was about 13.7 billion years ago and that stars formed 200 million years afterward (Bennett et al. 2003), it is reasonable to fix the model star formation at 12 Gyrs ago. It was assumed that the IMF does not vary as a function of time and galactic environment.

These results show that the LSBGs have a mix of old and young stellar populations with metallicities $Z = 0.0004 - 0.05$ and ages, or the e-folding time scale of star formation rate, $\tau = 0 - 16$ Gyrs. So the continuous range of colors, from very blue to very red, clearly shows that LSB galaxies at the present epoch define a wide range of evolutionary states. The HSBGs also show a similar trend in this optical-NIR color-color diagram although some of them show a bit redder colors. Although part of the low surface brightness galaxies are excluded when the 2MASS criteria is applied (see Sect.5.1), this qualitative conclusion of mixed population of LSBGs is still believable. Fig. 15a,b present the detected (Fig.a) and non-detected (Fig.b) LSBGs by 2MASS in the relation of $(U - B)$ vs. $(B - V)$, respectively. The contours show the 68.3% confidence level of the data points and the large squares in the center show their peaks. Although the 2MASS-detected galaxies are biased a bit to the population with redder colors than the non-detected ones by 2MASS, most of the detected ones (Sample-L2) still show a mix of young and old stellar populations since they belong to the “rest case” of stellar populations suggested by O’Neil et al. (1997a,b).

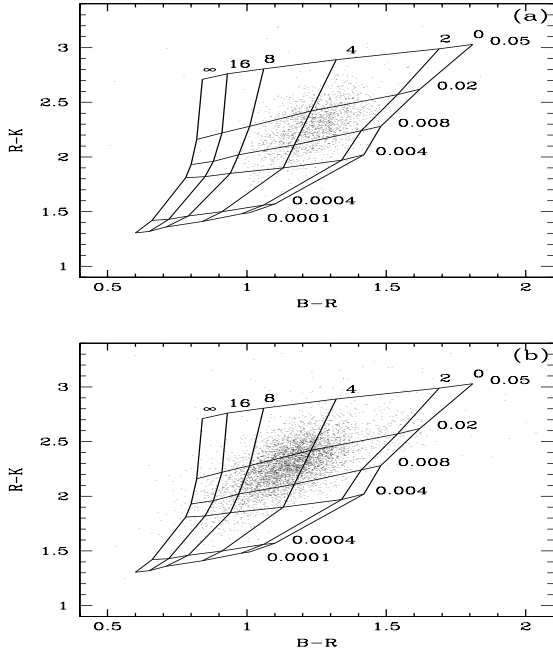


Figure 14. Trends in the $B - R$ and $R - K$ optical-NIR color-color diagram for Sample-L2 in (a), Sample-H2 in (b). The grids with different metallicities and ages are given by Bell et al. (2000) by using the GISSL98 implementation of the stellar population models of Bruzual & Charlot (2003).

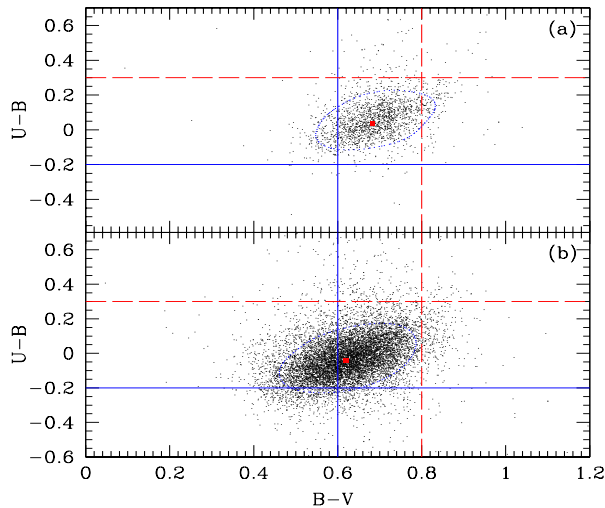


Figure 15. $U - B$ versus $B - V$ diagrams of the 2MASS-detected LSBGs (fig.a, our Sample-L2) and the non-detected ones (fig.b). The horizontal and vertical lines as in Fig. 10. The contours show the 68.3% confidence level of the data points and the large squares in the center show the peaks of them (please see the online color version for more details).

6.3 Color-magnitude diagrams

It was known that early-type galaxies in nearby clusters exhibit a tight color-magnitude relation (CMR), that is, more luminous early-type galaxies tend to have redder colors. This relation has been mainly ascribed to the metallicity effect (Chang et al. 2006a and the references therein).

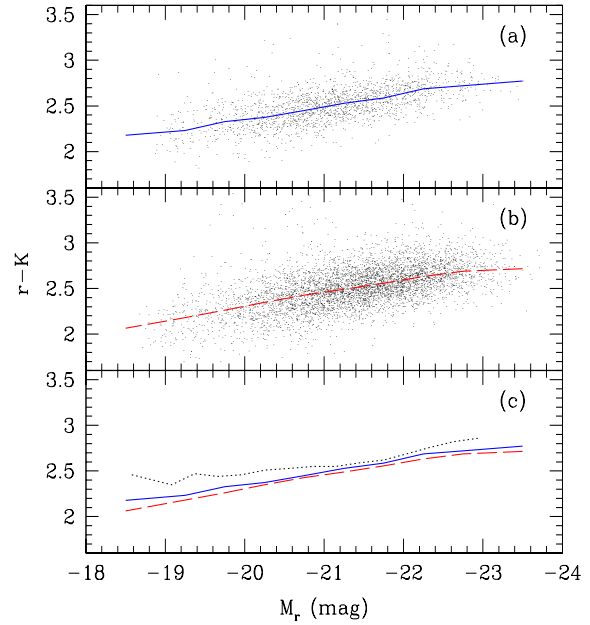


Figure 16. Color-magnitude relations of the sample galaxies. The optical-NIR $r - K$ color and the absolute magnitude in r -band M_r are contained: (a). Our sample of Sample-L2. (b). Our sample of Sample-H2. (c). It shows the comparisons among Sample-L2, (the solid line), Sample-H2, (the long-dashed line), and the results of Chang et al. (2006b, the dotted lines) for spiral galaxies.

The tight CMR of late-type galaxies have also been identified by many studies, such as Visvanathan & Grier-smith (1977), Blanton et al. (2003), Baldry et al. (2004), but with a different slope than the early-type galaxies. The optical-NIR CMR of spiral galaxies have been obtained for some samples. Chang et al. (2006b) present the CMR of a large sample of spiral galaxies selected from the SDSS and 2MASS. They found that the colors for faint galaxies have a very weak correlation with the luminosity, whereas the colors for bright galaxies are redder than those for less luminous galaxies. By comparing with stellar population synthesis model, they found that massive late-type galaxies have older and higher-metallicity stellar populations than those of less-massive galaxies.

In Fig. 16a we present the CMR for Sample-L2 for the relation of optical-NIR ($r - K$) colors and r -band absolute magnitudes M_r . Fig. 16b shows the same relations for Sample-H2. It seems there is no obvious difference between the LSBGs and the HSBGs in this relation, but the scatter of the HSBGs are a bit larger than those of the LSBGs. Both of them show that the brighter galaxies have redder colors than the less bright ones. Fig. 16c shows the comparisons among the results of Sample-L2, (the solid line), Sample-H2, (the long-dashed line), and that result of Chang et al. (2006b, the dotted line) for the SDSS spiral galaxies in the color-magnitude diagram. It shows the larger sample of spiral galaxies in Chang et al. (2006b) is a bit redder in ($r - K$) color than our samples at a given magnitude, which may be because we selected the galaxies with less bulge-component with $frac{Dev_r} < 0.25$, whereas they adopted < 0.5 , or these LSBGs had less star formation in the past. However, maybe

it is not very reliable to compare with Chang et al. (2006b) here since we did not exactly follow them to do the emission-line corrections for the CMR, because we think it strongly depends on models. However, the general trend of brighter galaxies showing redder ($r-K$) colors is real for these galaxies. Other colors, such as ($g-r$), ($r-i$), ($r-z$), ($r-J$), and ($J-K$), as presented in Chang et al. (2006b), also show a similar trend in their relations with M_r .

7 DISCUSSIONS AND CONCLUSIONS

Low surface brightness galaxies (LSBGs) are important populations in the Universe. They were studied little in the past due to the observational limits of their low surface brightness. The fantastic modern SDSS survey of large sky coverage area is unique for such studies because it detects as many low surface brightness galaxies. We select a large sample of 12,282 LSBGs from the main galaxy sample of SDSS-DR4 database, and present their basic properties in this paper. The results are summarized as follows.

(i) Firstly, we select 30,333 nearly face-on disk galaxies with $M_B < -18$ from the main galaxy sample of SDSS-DR4. Their surface brightness profiles can be fitted well by an exponential disk. The B -band central surface brightness of these disk galaxies distribute in a range of $18.5 < \mu_0(B) < 24.5$ mag arcsec $^{-2}$. This sample was then divided into two sub-samples: Sample-L (12,282, the LSBGs) and Sample-H (18,051, the HSBGs) by the surface brightness value of 22 mag arcsec $^{-2}$. The median $\mu_0(B)$ of Sample-L is 22.42 mag arcsec $^{-2}$ and the mean value is 22.50 mag arcsec $^{-2}$. The median and mean values of $\mu_0(B)$ of Sample-H are 21.41 and 21.29 mag arcsec $^{-2}$, respectively.

(ii) The scale length h of Sample-L are from 2 kpc to 19 kpc with the median scale length of 5.98 kpc. These values are similar to those scale lengths of Sample-H, which means that the LSBGs and HSBGs are comparable in size.

(iii) The absolute B -band magnitude M_B of Sample-L are from -18 to -23 mag with the median value of -20.08 mag and the mean value of -20.06 mag. These values are similar to those M_B of Sample-H (-20.47 and -20.41 mag respectively), which means that the LSBGs are not necessarily faint, and their luminosities are comparable to those of the HSBGs.

(iv) Some relations between the property parameters show the selection effects of the survey observations, such as the apparent magnitude vs. $\mu_0(B)$, distance versus $\mu_0(B)$, absolute magnitude versus $\mu_0(B)$, distance versus disk scale length, and the distance versus absolute magnitude. These relations show that the galaxies with higher surface brightness tend to be detected at farther distance; and the galaxies observed at farther distance are also brighter and have larger disk scale lengths.

(v) A fundamental correlation to the sample galaxies is the disk scale length $\log h$ versus absolute magnitude M_B . For Sample-L, the scale length $\log h$ and absolute magnitude M_B show very tight correlation, meaning that the brighter galaxies tend to be larger. The tight correlation between $\log h$ and M_B also exists in the HSBGs, but with a slightly steeper slope, which means that, at a given M_B , the observed LSBGs tend to be larger than the HSBGs, and for a given size of galaxies, the observed HSBGs tend to be brighter than the LSBGs.

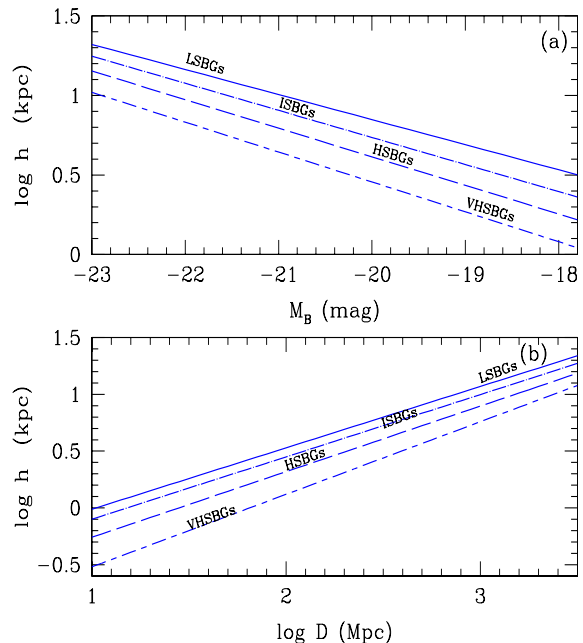


Figure 17. (a). Correlation of disk scale length and luminosity for the whole sample galaxies: LSBGs (the solid line); ISBGs (the dot-long dash line); HSBGs (the long-dash line); VHSBGs (the short-long dash line). (b). Correlation of disk scale length and distance of the whole sample galaxies, and the lines represent the same means as (a).

(vi) There is no obvious correlation between colors and central surface brightness $\mu_0(B)$ for our large sample of LSBGs. The correlation between colors and disk scale length ($\log h$) is weak even though it exists.

(vii) The color-color diagrams of ($U-B$) vs. ($B-V$) show that most of our LSBGs have a mix of young and old stellar populations. Following the definitions of O’Neil et al. (1997a,b), our sample may contain about 4.4% (535 out of 12282) “very blue” LSB galaxies with ($U-B$) <0.2 and ($B-V$) <0.6 , and $\sim 0.48\%$ (69 out of 12282) “very red” LSB galaxies with ($U-B$) >0.3 and ($B-V$) >0.8 . These fractions are 4.0% and 2.1% for our HSBGs, respectively.

(viii) A volume-limited sub-sample was extracted by considering $z < 0.1$ and brighter than the corresponding M_r , which is complete and can be used to check the incompleteness of surface brightness (especially at the low end), and to check how the property relations change. The only one with obvious change is the relation of $\log h$ versus $\mu_0(B)$, which shows a correlation in this sub-sample.

(ix) The optical-NIR color-color diagrams can break the degeneracy of age and metallicity. By doing cross-correlations between the SDSS and 2MASS datasets, we obtain the NIR color sample of Sample-L2 (15.29% of the Sample-L), and such sample of Sample-H2 (29.47% of the Sample-H). The smaller detected fraction of LSBGs is not unexpected.

The color-color diagram of ($R-K$) vs. ($B-R$) clearly shows the stellar populations of the sample galaxies by comparing with the predictions of the stellar population synthesis models. This shows that our LSBG samples have a wide range of ages and metallicities, from $Z=0.0004$ to $Z=Z_\odot$,

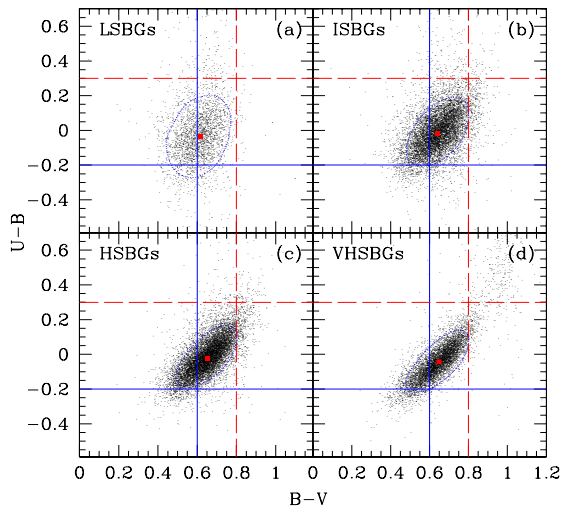


Figure 18. $U-B$ versus $B-V$ diagram: (a). LSBGs, (b). ISBGs, (c). HSBGs, (d). VHSBGs. The horizontal and vertical lines are the same as in Fig. 10. The contours and the squares are the same as in Fig. 15 (please see the online color version for more details).

even $Z=0.05$, and the exponential infall time-scale τ is from 0 to 16 Gyrs. It confirms that most LSBGs have a mix of young and old stellar populations.

(x) The color-magnitude relations ($(r-K)$ vs. M_r) of our LSBGs confirm that there exist the CMR for the spiral galaxies with low surface brightness, showing that the brighter LSBGs tend to be redder. And, the HSBGs do not show obvious differences from the LSBGs on their CMRs.

(xi) We have attempted to divide our total nearly face-on disk galaxies (30,333) into four sub-groups according to their surface brightness by following McGaugh (1996): the VHSBGs with $\mu_0(B) < 21.25$ mag arcsec $^{-2}$, the HSBGs with $21.25 < \mu_0(B) < 22$ mag arcsec $^{-2}$, the ISBGs with $22 < \mu_0(B) < 22.75$ mag arcsec $^{-2}$ and the LSBGs with $22.75 < \mu_0(B) < 24.5$ mag arcsec $^{-2}$. Similar to the comparisons between LSBGs and HSBGs in Sect. 4, these four sub-groups do show obvious difference in the relations of $\log h$ vs. M_B , $\log h$ vs. $\log D$, and some difference in the color-color diagram of $(U-B)$ vs. $(B-V)$ as given in Fig. 17 and Fig. 18. Fig. 17a shows that, at a given M_B or scale length $\log h$, the observed galaxies in the four sub-groups show the gradual increase in their scale length or gradual decrease in their luminosity following the decreasing surface brightness. The four lines refer to the linear least-square fits for the data in the four sub-groups. To show the scatter of the data as well, we obtained their standard derivations as 0.057, 0.049, 0.050, 0.093 dex for the LSBGs, ISBGs, HSBGs and VHSBGs, respectively. Fig. 17b also shows such gradual changes in their relations of scale length and distance. Similarly, the four lines refer to the linear least-square fits for the data in the four sub-groups, and the standard derivations of the data to the fittings are 0.092, 0.096, 0.098, 0.13 dex for the LSBGs, ISBGs, HSBGs and VHSBGs, respectively. Fig. 18a-d presents the discrepancies between their stellar populations among the four sub-groups. Even with large scatter, the LSBGs do generally show slightly bluer $(B-V)$ color than others, and there are almost no the “red populations” in

the LSBGs. It also shows the VHSBGs consist of more “red populations” than other groups. The counters refer to the 68.3% confidence level of the data points, which show the gradually redder $(B-V)$ colors of the sub-groups following their increasing surface brightness.

In summary, this large sample (12,282) of LSBGs greatly extends the known sample of LSBGs up to date. This is the first paper of our series work about the large sample of LSBGs to present the distributions of some property parameters of them, and to provide more information about some of their fundamental properties, e.g. the tight correlations between $\log h$ and M_B , $\log h$ and $\log D$, moreover, it presents their stellar populations by using the color-color diagrams of them.

In the following work, we will discuss more about the major issues of these “populations”, such as why they are LSBGs with small star formation rates, what is their total mass content and M/L ratios, and what is their total contribution to the baryonic/total mass etc. We will also obtain their metallicities in interstellar gas from emission lines. The detailed surface photometry and color gradients will be also studied in detail. Moreover, some more efforts on other aspects are also needed, such as to extend the studies of edge-on galaxies, but the dust effects must be considered carefully then.

ACKNOWLEDGMENTS

We thank our referee for the valuable comments and suggestions, which help to improve well our work. We thank Ruixiang Chang, Zhengyi Shao, Jianling Wang for helpful discussions, and thank James Wicker for English corrections on the text. We thank the NSFC grant support under Nos. 10403006, 10433010, 10673002, 10573022, 10333060, and 10521001, and the National Basic Research Program of China (973 Program) No.2007CB815404, 06 and the Doctoral Foundation of SYNU of China (054-55440105020).

REFERENCES

- Abazajian K. et al., 2003, AJ, 126, 2081
- Abazajian K. et al., 2004, AJ, 128, 502
- Baldry I. K., Glazebrook K., Brinkmann J., Ivezić Z., Lupton R. H., Nichol R. C., Szalay A. S., 2004, ApJ, 600, 681
- Beijersbergen M., de Blok W., van der Hulst J., 1999, A&A, 351, 903
- Bell E. F., Barnaby D., Bower R. G., de Jong R. S., Harper D. A., Hereld M., Loewenstein R. F., Rauscher B. J., 2000, MNRAS, 312, 470
- Bell E. F., Bower R. G., de Jong R. S., Hereld M., Rauscher B. J., 1999, MNRAS, 302, L55
- Bell E. F., de Jong R. S., 2000, MNRAS, 312, 497
- Bennett C. et al., 2003, ApJS, 148, 1
- Bergvall N., Ronnback J., Masegosa J., Ostlin G., 1999, A&A, 341, 697
- Bernardi M., Sheth R. K., Nichol R. C., Schneider D. P., Brinkmann J., 2005, AJ, 129, 61
- Blanton M. R. et al., 2003, AJ, 125, 2348
- Blanton M. R. et al., 2005, AJ, 129, 2562

- Boissier S. et al., 2008, *ApJ*, 681, 244
- Boissier S., Monnier Ragaigine D., Prantzos N., van Driel W., Balkowski C., O’Neil K., 2003, *MNRAS*, 343, 653
- Bothun G. D., 1982, *ApJS*, 50, 39
- Bothun G. D., Geller M., Kurtz M., Huchra J., Schild R., 1992, *ApJ*, 395, 349
- Bothun G. D., Impey C., McGaugh S., 1997, *PASP*, 109, 745
- Bothun G. D., Impey C. D., Malin D. F., Mould J. R., 1987, *AJ*, 94, 23
- Bruzual G., Charlot S., 2003, *MNRAS*, 344, 1000
- Burkholder V., Impey C., Sprayberry D., 2001, *AJ*, 122, 2318
- Caldwell N., Bothun G. D., 1987, *AJ*, 94, 1126
- Chang R. X., Gallazzi A., Kauffmann G., Charlot S., Ivezić Z., Brinchmann J., Heckman T. M., 2006a, *MNRAS*, 366, 717
- Chang R. X., Shen S. Y., Hou J. L., Shu C. G., Shao Z. Y., 2006b, 372, 199
- Chen et al., 2008, (in preparation)
- Cutri R. M. et al., 2000, Explanatory Supplement to the 2MASS Second Incremental Data Release (Pasadena: Caltech)
- de Blok W. J. G., McGaugh S. S., 1997, *MNRAS*, 290, 533
- de Blok W. J. G., McGaugh, S. S., van der Hulst J. M., 1996, *MNRAS*, 283, 18
- de Blok W. J. G., van der Hulst J. M., 1998a, *A&A*, 335, 421
- de Blok W. J. G., van der Hulst J. M., 1998b, *A&A*, 336, 49
- de Blok W. J. G., van der Hulst J. M., Bothun G. D., 1995, *MNRAS*, 274, 235
- Disney M. J., 1976, *Nature*, 263, 573
- Disney M. J., Phillips S., 1983, *MNRAS*, 205, 1253
- Ellis G., Grayson E., Bond H. E., 1984, *PASP*, 96, 283
- Freeman K. C., 1970, *ApJ*, 160, 811
- Galaz G., Dalcanton J., Infante L., Treister E., 2002, *AJ*, 124, 1360
- Galaz G., Villalobos A., Infante L., Donzelli C., 2006, *AJ*, 131, 2035
- Han M., 1992, *ApJS*, 81, 35
- Heller A. B., Brosch N., 2001, *MNRAS*, 327, 80
- Hinz, J. L. et al. 2007, *ApJ*, 663, 895
- Hogg, D. W. et al., 2004, *ApJ*, 601, L29
- Huchra J. P., 1977, *ApJS*, 35, 171
- Impey C. D., Bothun G. D., 1997, *ARA&A*, 35, 267
- Impey C. D., Burkholder V., Sprayberry D., 2001, *AJ*, 122, 2341
- Impey C. D., Sprayberry D., Irwin M. J., Bothun G. D., 1996, *AJ*, 105, 209
- Jarrett T. H., Chester T., Cutri R., Schneider S., Rosenberg J., Huchra J. P., Mader J., 2000a, *AJ*, 120, 298
- Jarrett T. H., Chester T., Cutri R., Schneider S., Skrutskie M., Huchra J. P., 2000b, *AJ*, 119, 2498
- Kniazev A. Y., Grebel E. K., Pustilnik S. A., Pramskij A. G., Kniazeva T. F., Prada F., Harbeck D., 2004, *AJ*, 127, 704
- Lauberts A., Valentijn E. A., 1989, *The Surface Photometry Catalogue of the ESO-Uppsala Galaxies*. ESO
- Liang et al., 2008, (in preparation)
- MacArthur L. A., Courteau S., Bell, E. F., Holtzman J. A., 2004, *ApJS*, 152, 175
- McGaugh S. S., 1994, *ApJ*, 426, 135
- McGaugh S. S., 1996, *MNRAS*, 280, 337
- McGaugh S. S., Bothun G. D., 1994, *AJ*, 107, 530
- McGaugh S. S., de Blok W. J. G., 1997, *ApJ*, 481, 689
- McGaugh S. S., Schombert J. M., Bothun G. D., 1995, *AJ*, 109, 2019
- McIntosh D. H., Bell E. F., Weinberg M. D., Katz N., 2006, *MNRAS*, 373, 1321
- Mei, L., Yuan, W. M., Dong, X. B., 2008, *ChJAA* (in press)
- Monnier-Ragaigine D., van Driel W., Schneider S., Jarrett T., Balkowski C., 2003, *A&A*, 405, 99
- Morshidi-Esslinger, Z., Davies, J. I., Smith, R. M., 1999, *MNRAS*, 304, 297
- Morshidi-Esslinger, Z., Davies, J. I., Smith, R. M., 1999, *MNRAS*, 304, 311
- O’Neil K., Bothun G. D., Cornell M., 1997a, *AJ*, 113, 1212
- O’Neil K., Bothun G. D., Schombert J., 1998, *AJ*, 116, 2776
- O’Neil K., Bothun G. D., Schombert J., Cornell M. E., Impey C. D., 1997b, *AJ*, 114, 2448
- Pizzella A., Corsini E. M., Sarzi M., Magorrian J., Mendez-Abreu J., Coccato L., Morelli L., Bertola F., 2008, *MNRAS*, 387, 1099
- Romanishin W., Krumm N., Salpeter E., Knapp G., Strom K., Strom S. 1982, *ApJ*, 263, 94
- Romanishin W., Strom K. M., Strom S. E., 1983, *ApJ*, 263, 94
- Sandage A., Binggeli B., 1984 *AJ*, 89, 919
- Schlegel D. J., Finkbeiner D. P., Davis M., 1998, *ApJ*, 500, 525
- Schombert J. M., Bothun G. D., 1988, *AJ*, 95, 1389
- Schombert J. M., Bothun G. D., Schneider S. E., McGaugh S. S., 1992, *AJ*, 103, 1107
- Shao Z. Y., Xiao Q. B., Shen S. Y., Mo H.J., Xia X. Y., Deng Z. G., 2007, *ApJ*, 659, 1159
- Skrutskie M. F. et al., 1997, in *The Impact of Large Scale Near-IR Sky Surveys*, ed. F. Garzon, N. Epchtein, A. Omont, W. B. Burton, & P. Persi (Dordrecht: Kluwer), 25
- Smith J. A. et al., 2002, *AJ*, 123, 2121
- Sprayberry D., Impey C. D., Irwin M. J., 1996, *ApJ*, 463, 535
- Sprayberry D., Impey C. D., Irwin M. J., Bothun G. D., 1997, *ApJ*, 482, 104
- Stoughton C. et al., 2002, *AJ*, 123, 485 (SDSS EDR paper)
- Strauss M. et al., 2002, *AJ*, 124, 1810
- Tinsley B., 1978, *ApJ*, 222, 14
- van der Hulst J. M., Skillman E. D., Smith T. R., Bothun G. D., McGaugh S. S., de Blok W. J. G., 1993, *AJ*, 106, 548
- van Zee L., Haynes M. P., Salzer J. J., 1997, *AJ*, 114, 2497
- Visvanathan N., Griersmith D., 1977, *A&A*, 59, 317
- York D. et al., 2000, *AJ*, 120, 1579
- Zackrisson E., Bergvall N., Ostlin G., 2005, *A&A*, 435, 29
- Zhong et al., 2008, (in preparation)
- Zwicky F., 1957, in *Morphological Astronomy* (New York, Springer-Verlag)